Skeletal trade-offs in coralline algae in response to ocean acidification

SJ McCoy[1]★ and F Ragazzola[2]

[1]Department of Ecology and Evolution, The University of Chicago, Chicago, IL 60637, USA. Present Affiliation: Plymouth Marine Laboratory, Prospect Place, The Hoe, Plymouth PL1 3DH, UK.

[2]Department of Earth Science, University of Bristol, Wills Memorial Building, Queen's Road, Clifton B38 1RJ, UK.

★e-mail: mccoy@uchicago.edu

Introduction

Ocean acidification is changing the marine environment, with potentially serious consequences for many organisms. Much of our understanding of ocean acidification effects comes from laboratory experiments, which demonstrate physiological responses over relatively short timescales[1-10]. Observational studies and, more recently, experimental studies in natural systems suggest that ocean acidification will alter the structure of seaweed communities[11-13]. Here, we provide a mechanistic understanding of altered competitive dynamics among a group of seaweeds, the crustose coralline algae (CCA). We compare CCA from historical experiments (1981-1997) with specimens from recent, identical experiments (2012) to describe morphological changes over this time period, which coincides with acidification of seawater in the Northeastern Pacific[14-16]. Traditionally thick species decreased in thickness by a factor of 2.0-2.3, but did not experience a change internal skeletal metrics. In contrast, traditionally thin species remained approximately the same thickness but reduced their total carbonate tissue by making thinner inter-filament cell walls. These changes represent alternative mechanisms for the reduction of calcium carbonate production in CCA and suggest energetic trade-offs related to the cost of building and maintaining a calcium carbonate skeleton as pH declines. Our classification of stress response by morphological type may be generalizable to CCA at other sites, as well as to other calcifying organisms with species-specific differences in morphological types.

Main Text

Coralline algae are globally distributed seaweeds that accrete a calcified skeleton and are associated with high-disturbance habitats across global ecosystems, including areas with high grazing pressure, intense wave action, or low-light[17]. Crustose coralline algae (CCA) provide

settlement substrates and signals as well as nursery habitat functions for a variety of coastal organisms, including corals, starfish, and fishes[18,19], and thus corallines' fates could be closely tied to those of productive coastal systems worldwide.

As both photosynthesizers and calcifiers, coralline algae may respond in multiple ways to ocean acidification and have received much attention as potential 'first indicator' species. Growth, photosynthesis, and calcification initially increase with declining pH and concomitant increasing availability of bicarbonate (HCO_3^-) for photosynthesis, followed by a decline in growth and calcification associated with decreased seawater carbonate (CO_3^{2-}) availability for calcification as pH continues to fall[1,20]. The expected parabolic relationship between declining pH and coralline fitness may explain the varied responses to declining pH and pCO_2 that have been recorded to date[2-8,21].

Results from experimentally elevated pCO_2 (increased acidification) show diverse patterns, including reduced coralline algal growth and tissue integrity and increased the likelihood of dissolution and tissue necrosis[2-6], no effect of pCO_2 on algal growth parameters[7], and even increased inorganic carbon fixation, photosynthesis, and calcification with increased DIC[8]. Furthermore, there is evidence that coralline algae from habitats more variable in pH appear more robust in experimentally elevated pCO_2 conditions[6,8].

Growth and morphological traits that influence ecological outcomes confer greater fitness on individuals with fast growth or thick thalli (algal individuals)[22], both of which are traits that rely on accretion of calcium carbonate. Temperate CCA compete with one another for space in the

kelp understory through a series of overgrowth interactions, and the outcome depends strongly on morphology and growth strategy [22-25]. Rapid lateral growth is important for occupying bare space, thickness at the growing edge is the strongest determinant of competition, and overall thicker species are favored in the presence of grazers[22,24]. Fast lateral growth and increased thickness appear to trade-off, as they do not co-occur in any one species[24], likely due to energetic constraints that incur higher maintenance costs for thick crusts and resources needed for rapid growth.

Previous work has shown that in the Northeast Pacific, competitive interactions and community structure among CCA have changed over 30 years, in ways predictable from pH decline[13,23]. We examine morphological change in this community by comparing individuals over time. Of four CCA species that co-occur and compete in the intertidal zone in the northeast Pacific, we show that all now maintain less skeletal material than in the past, but the response depends on morphological type.

We examined three metrics of the calcareous skeleton of the CCA *Lithophyllum impressum, Lithothamnion phymatodeum, Pseudolithophyllum muricatum*, and *Pseudolithophyllum whidbeyense*. Individuals were collected at Tatoosh Island, WA in the Northeast Pacific from plots kept grazer-free for approximately 2 years prior to specimen collection. Specimens were photographed using scanning electron microscopy (SEM) to determine thickness of the algal thallus and the thicknesses of inter- and intra-filament cell walls for each species.

To determine change over time, we compared the historical measurements (1981-1997) to

82 modern specimens (2012) collected from the same populations at Tatoosh Island (historical
83 baselines reported in Supplementary Information, Section A). We observed changes in thallus
84 thickness over this interval, related to morphological groupings (Fig. 1). Historical specimens of
85 *L. impressum* and *P. muricatum* were 2-2.3 times thicker than modern individuals, both on
86 average across the thallus ($p<0.001$) and specifically at the growing margin ($p<0.05$), the edge
87 tissue involved in active growth an important in overgrowth interactions. *L. phymatodeum* and *P.*
88 *whidbeyense*, both historically thinner than *L. impressum* and *P. muricatum*, showed mixed
89 responses in thallus thickness. *L. phymatodeum* thinned overall, with historical specimens 1.3
90 times thicker than modern, but showed no response specifically at the growing edge. In contrast,
91 *P. whidbeyense* was historically 1.8 times thicker than modern at the growing edge, but showed
92 no change in overall thickness (details for all species reported in Supplementary Information,
93 Section B).
94
95 Inter-filament cell walls thinned over time in both *L. phymatodeum* (Mann-Whitney
96 $U(67)=327.0$, $p=0.025$) and *P. whidbeyense* ($t(144)=2.023$, $p=0.025$). Changes in inter-filament
97 cell walls were not observed in *L. impressum* ($t(144)=-1.690$, $p=0.093$) and *P. muricatum*
98 (Mann-Whitney $U(96)=932.0$, $p=0.108$). No changes were observed in the intra-filament cell
99 walls of any species over time (Fig. 2, details in Supplementary Information Section C).
100
101 Coralline algae have received scientific scrutiny in the context of ocean acidification due to their
102 importance for maintaining local biodiversity, their influence on the coastal carbon cycle, and
103 their potentially high susceptibility to ocean acidification. It is thus essential to understand
104 acidification-induced changes to their skeletal morphology and its effect on ecological function.

105 The rate at which conditions change has been shown to be important in laboratory studies of
106 coralline algal responses to acidification[9]. Testing for responses to acidification using field-
107 grown specimens accounts for acclimatisation of individuals and populations to a stressor as it is
108 gradually introduced over time. At our study site, a pH decline of 0.058 units yr^{-1} has been
109 recorded since 2000[14,15] and isotopic evidence from mussel shells indicate the onset of
110 unprecedented changes in carbonate chemistry over the last 30 years[16] in the absence of changes
111 to other environmental parameters including temperature and upwelling regime[14-16] (Fig. 3). Our
112 data suggest that current field populations have already made energetic adjustments to cope with
113 increased acidity in this region.
114
115 In response to ocean acidification and concurrent decrease in the saturation of carbonate in
116 seawater, a reduction in the net quantity of calcium carbonate ($CaCO_3$) skeletal material is
117 expected. $CaCO_3$ amount could be reduced by simply changing the mineral density (quality), or
118 also by reducing the thickness of cell walls (quantity). Both of these mechanisms reduce the
119 structural strength of coralline tissue[3] and may have ecological implications, for example in the
120 case of physical disturbances, endophytic biota, or heavy grazing. In the thin, fast-growing
121 species *L. phymatodeum* and *P. whidbeyense*, we observed a reduction in the thickness of inter-
122 filament cell walls. These walls are arranged longitudinally within the algal individual (Fig. 2c),
123 meaning that inter-filament cell walls form as an individual grows laterally. Therefore,
124 decreasing the thickness of inter-filament cell walls likely reduces the cost of lateral growth in
125 species of the thin morphological type, perhaps allowing the organism to present the same
126 surface area for photosynthesis and maintain rapid lateral growth rates while reducing the
127 structural cost (Supplementary Fig. S1-4). On the other hand, reduced $CaCO_3$ production

achieved by less total growth is concordant with the morphological changes observed in thick, slow growing species in this study (Fig. 1), which we attribute to the larger energetic burden of maintaining a thick skeleton in lower-pH conditions.

This second mechanism may more directly affect algal ecology via competitive overgrowth interactions. In particular, decreased thickness of the growing margin will translate to a reduced competitive ability, as has been shown in the case of *P. muricatum*[13,26]. This species was formerly dominant in abundance and competitive ability in areas where grazers had been experimentally removed and also in unmanipulated communities[23]. Modern data indicates a reversal, where *P. muricatum* now wins less than half of its competitive interactions both with and without grazers, compared with 100% previously[13]. By testing specimens from these same competitive experiments in the 1980s-1990s[23] and 2010s[13], we have linked observed ecological change to a morphological mechanism. Changes in *P. muricatum* have been the clearest to identify thus far due to the particular ecological importance of this species. However, we predict that *L. impressum* may be the next to show observable changes based on the morphological data we have collected here. Due to the strong ecological dominance of a single species previously observed in this community, we hypothesize that competitive release may cause other CCA species to increase in abundance in the near-term. Long-term community dynamics will ultimately depend on the severity of climate change as well as the degree of structural reduction of CCA skeletons that could increase species' susceptibility to physical disturbances.

Recent laboratory studies of the coralline alga *Lithothamnion glaciale* revealed phased responses to elevated pCO_2 over exposure time. After 3 months, individuals cultured under high pCO_2

showed a reduction in cell (inter- and intra-filament) wall thickness while growth rate was maintained[3]. After 10 months, however, there was a reduction in growth at all elevated pCO_2 but the cell wall thickness was maintained with respect to control specimens, as well as the volume-normalised amount of calcite deposited[10]. These results reveal different phases during acclimatisation with a different mechanistic response in cell wall thickness and growth rate, which highlight the importance of conducting long-term studies, whether in the field or in the laboratory, and also suggest a potential sequence of trade-offs experienced as organisms begin to feel the energetic constraints of acidification stress. In the species studied here, ocean acidification appears to be more stressful to thicker species, which contain greater amounts of skeletal $CaCO_3$ per unit photosynthetic tissue (Supplementary Fig. S3, S4). Therefore, thicker species likely require an energetic response sooner than their thinner counterparts, and may thus be further along a potential trade-off sequence in present day seawater conditions.

Recent studies have also shown the importance of including natural environmental variability in acidification due to the large diurnal variations in pH and pCO_2 experienced in kelp forest and coral reef environments[21,27]. Individuals living in a more variable habitat have been shown to be better acclimatised to changes in pCO_2 within the scope of the natural variability where an individual originated[6,21]. However, this is coupled with the finding that variable treatments exacerbate the effects of elevated pCO_2 compared to constant treatments with the same mean pCO_2[27]. Our study reports findings from a 30-year comparison of field specimens from a kelp-dominated shoreline, with large diurnal fluctuations in pH[14,15], and therefore takes into account environmental variability as well as the gradual timescale of acidification in natural systems.

While elevated water temperature has been neither observed nor predicted in the Northeastern Pacific, this phenomenon is of global concern in concert with acidification. Warmer temperatures boost growth and calcification rates in coralline algae[2,28], yet reduces the proportion of tissue that consists of $CaCO_3$ material and effectively reduces skeletal density as cells produced under elevated temperatures are less-extensively calcified[28]. Therefore, it is uncertain whether the elevated growth rates afforded by rising seawater temperatures can effectively 'rescue' observed declines in skeletal metrics engendered by ocean acidification.

In this study, we have identified a morphology-dependent response to ocean acidification in CCA, which underlies changes in the competitive abilities of these species in the field between the 1980s and 2010s[13]. The mechanisms we have identified in crustose coralline algae may be applicable to other calcifying taxa with species-specific differences in morphological types dictated by skeletal thickness and growth rates. Corals are another example of "photosynthetic" organisms that abound in morphological forms[29]. Variation in growth rates, skeletal thickness, and branching alter the ratio of surface area to calcium carbonate skeletal volume, which is an energetic sink under acidification scenarios. Previous work has shown ocean acidification effects on sclerodermites, or groups of calcified fibers in the coral skeleton within septa, among coral recruit[30]. We suggest that future work look for trade-offs between coral growth and the structure of septa, which may be analogous to intra- and interfilament cell wall structures. Due to variation in calcification patterns, growth, and structure among organisms and species, it is important to find morphological classifications to describe patterns of stress response to climate stressors such as ocean acidification. This method may be valuable as a more generalizable rule than studying individual responses at the species level.

197

198 **Methods**

199 *Study Site and Physical Data*

200 *In situ* pH, as well as a suite other environmental parameters including temperature, chl *a*,
201 salinity, and dissolved oxygen[14,15] has been recorded at Tatoosh Island, WA, USA in the
202 Northeast Pacific (48.4°N, 128.7°W) since 2000. This data revealed a decline in pH of 0.058
203 units per year at Tatoosh Island[14,15]. Further, local seawater carbon chemistry near Tatoosh
204 Island has been reconstructed from mussel shells back to 663 A.D., and indicated the onset of
205 these rapid changes in inorganic carbon chemistry occurred only over the last several decades
206 relative to historical baselines[16]. These changes in pH and inorganic carbon cycling have
207 occurred in the absence of other changes to the seawater environment, including changes in
208 temperature, nutrients, or upwelling[15,16]. Therefore, we have strong evidence that seawater
209 inorganic carbon chemistry and pH have changed rapidly and in isolation over the last 30 years
210 and intensified since 2000 at Tatoosh Island (Fig. 3).

211

212

213 *Sample Collection*

214 At Tatoosh Island, specimens of *Lithophyllum impressum* Foslie*, Lithothamnion phymatodeum*
215 Foslie*, Pseudolithophyllum muricatum* (Foslie) Steneck & R.T. Paine, and *Pseudolithophyllum*
216 *whidbeyense* (Foslie) Steneck & R.T. Paine were transplanted onto artificial marine epoxy
217 substrate (Sea Goin' Poxy Putty, Permalite Plastics, Inc., Rancho Dominguez, CA) by chiseling
218 pieces >1.5 cm^2 from the surrounding rock and embedding the sample into a flattened disc of wet
219 epoxy *sensu* Paine[23]. Archival samples (*L. impressum,* n=5, 1981, 1981, 1993, 1994, 1997; *L.*

220 *phymatodeum*, n=3, 1981, 1993, 1997; *P. muricatum*, n=5, 1981, 1982, 1993, 1994, 1997; *P.*
221 *whidbeyense*, n=6, 1981, 1981, 1981, 1993, 1994, 1997) from previous transplants were
222 preserved as dry specimens at the University of Washington, and were provided by R.T. Paine.
223 Modern samples (*L. impressum,* n=6; *L. phymatodeum*, n=6; *P. muricatum*, n=6; *P. whidbeyense*,
224 n=6) were transplanted in 2010 and collected in 2012, and were conducted with identical
225 methods as previous transplants, described above. Individuals were taken from the same
226 populations and location at Hedophyllum Cove on Tatoosh Island for historical and modern
227 transplants and collections. Individuals were collected at approximately 0 m MLLW (mean
228 lowest low water) and all transplants were placed at exactly 0 m MLLW in historical and modern
229 experiments. Both archival and modern specimens were dried in the shade for 48 hours, and
230 subsequently stored dry in the laboratory. All samples were grown in Hedophyllum Cove on
231 Tatoosh Island for approximately 2 years, and collected during the spring (April-June).
232 Specimens were grown in plots with grazers experimentally removed (manual removals) to
233 control for confounding effects of grazing on thallus thickness and structure[13,23]. Growth rates
234 were measured from digital photographs of transplants using ImageJ analysis software
235 (http://imagej.nih.gov/ij/).
236
237 *SEM Measurements and Analysis*
238 For SEM analysis, archival and modern dried thalli were sectioned perpendicular to the axis of
239 maximum growth, at the growing edge. Samples of *P. muricatum* were mounted on aluminum
240 stubs and coated with 8 nm palladium for analysis on an FEI Nova NanoSEM 230 at the
241 University of Chicago Materials Research Center. Samples of *L. impressum, L. phymatodeum,*
242 and *P. whidbeyense* were mounted on aluminum stubs and coated with 20 nm gold for analysis

243 on a Hitachi S-3500N SEM at the University of Bristol.

244

245 Using digital SEM photographs, we measured the intra- and inter-filament cell wall thickness
246 (within and between cell layers, respectively; Fig. 2c)[10]. Measurements were made in three cells
247 from the growth edge to avoid newly deposited material that may not be fully calcified. These
248 measurements were performed using ImageJ analysis software. To quantify baseline species
249 differences in historical samples, we used ANOVA and Tukey's HSD Post-Hoc text. We used
250 Welch's t-test to look for differences between treatments in for cell wall thicknesses. *L.*
251 *phymatodeum* and *P. muricatum* cell wall data were non-normally distributed, so we performed a
252 Mann-Whitney Rank Sum Test to test for differences over time in those species.

253

254 Fractional calcite density was measured using Image J analysis software
255 (http://imagej.nih.gov/ij/). Calcite density, defined here as the fractional area within a digital
256 quadrat composed of calcite-bearing structures[28], was determined by transforming cross-
257 sectional SEM micrographs taken at high magnification (2,500x) into black and white images to
258 measure relative surface areas of calcified tissue and interstitial cellular space of the cross
259 section[26]. Calcite density was compared between archival and modern samples over all four
260 species using ANOVA (Supplementary Fig. S3).

261

262 Thallus thickness along transects starting at the growing edge was also measured using digital
263 SEM photographs[26]. Thickness of each algal thallus, or individual, was measured at 33-µm
264 intervals using ImageJ analysis software. To quantify baseline species differences in historical
265 samples, we used ANOVA and Tukey's HSD Post-Hoc text, and we performed a two-tailed t-

test to identify differences in average thallus thickness over time. All thickness and cell wall data is available in the Pangaea database (Pangaea.de), Issue #PDI-7649.

Acknowledgments

We would like to thank RT Paine for making his archival coralline algal specimens available for tissue analysis, Q Guo for assistance on the SEM at the University of Chicago Materials Research Science and Engineering Center, FB McCoy for clerical assistance, and the Makah Tribe for access to Tatoosh Island and permission to conduct field research. RT Paine, CA Pfister, T Price, and JT Wootton provided helpful comments. SJM would like to acknowledge research funding provided by the United States National Science Foundation Doctoral Dissertation Improvement Grant DEB-1110412 (CA Pfister and SJM), the Achievement Rewards for College Scientists Foundation, and United States Government support under and awarded by DoD, Air Force Office of Scientific Research, National Defense Science and Engineering Graduate Fellowship, 32 CFR 168a, and by the United States National Science Foundation Graduate Research Fellowship, Grant No. 1144082. The United States National Science Foundation OCE-09-28232 (CA Pfister) and DEB-09-19420 (JT Wootton) funded Tatoosh research. FR would like to acknowledge the support of the Leverhulme Trust, RJ5540.

Author contributions

SJM collected field specimens and designed the experiment. FR took SEM photos. SJM and FR took measurements, analyzed, and discussed the data. SJM wrote the manuscript with contributions from FR.

289 **References**

290 1. J. B. Ries, A. L. Cohen, D. C. McCorkle, Marine calcifiers exhibit mixed responses to CO_2-
291 induced ocean acidification. *Geol.*37:1131–1134 (2009).
292
293 2. S. Martin, J.-P. Gattuso, Response of Mediterranean coralline algae to ocean acidification and
294 elevated temperature. *Global Change Biol.* **15**, 2089–2100 (2009).
295
296 3. F. Ragazzola *et al.* Ocean acidification weakens the structural integrity of coralline algae.
297 *Global Change Biol.* **18**, 2804–2812 (2012).
298
299 4. J. Büdenbender, U. Riebesell, A. Form, Calcification of the Arctic coralline red algae
300 *Lithothamnion glaciale* in response to elevated CO_2. *Mar. Ecol. Prog. Ser.* **441**, 79–87 (2011).
301
302 5. H. L. Burdett *et al.* The effect of chronic and acute low pH on the intracellular DMSP
303 production and epithelial cell morphology of red coralline algae. *Mar. Biol. Res.* **8**, 756–763
304 (2012).
305
306 6. F. Noisette, H. Egilsdottir, D. Davoult, S. Martin, Physiological responses of three temperate
307 coralline algae from contrasting habitats to near-future ocean acidification. *J. Exp. Mar. Biol.*
308 *Ecol.* **448**, 179–187 (2013).
309
310 7. H. Egilsdottir, F. Noisette, L. M. L. J. Noël, J. Olafsson, S. Martin, Effects of pCO_2 on
311 physiology and skeletal mineralogy in a tidal pool coralline alga *Corallina elongata. Mar. Biol*.
312 **160**, 2103-2112 (2013).
313
314 8. K. Gao *et al.* Calcification in the articulated coralline alga *Corallina pilulifera*, with special
315 reference to the effect of elevated CO_2 concentration. *Mar. Biol.* **177**, 129-132 (1993)
316
317 9. N. A. Kamenos *et al.* Coralline algal structure is more sensitive to rate, rather than the
318 magnitude, of ocean acidification. *Global Change Biol.* **19**, 3621-3628 (2013).
319
320 10. F. Ragazzola *et al.* Phenotypic plasticity of coralline algae in a high CO_2 world. *Ecology and*
321 *Evolution* **3**, 3436-3446 (2013).
322
323 11. L. Porzio, M. B. Buia, J. M. Hall-Spencer, Effects of ocean acidification on macroalgal
324 communities. *J. Exp. Mar. Biol. Ecol.* **400**, 278-287 (2011).
325
326 12. K. J. Kroeker, F. Micheli, M. C. Gambi, Ocean acidification causes ecosystem shifts via
327 altered competitive interactions. *Nature Clim. Change*, **3**, 156-159 (2013).
328
329 13. S. J. McCoy, C. A. Pfister, Historical comparisons reveal altered competitive interactions in
330 a guild of crustose coralline algae. *Ecol. Lett.*, **17**, 475-483 (2014).
331
332 14. J. T. Wootton, C. A. Pfister, J. D. Forester, Dynamic patterns and ecological impacts of
333 declining ocean pH in a high-resolution multi-year dataset. *Proc. Natl. Acad. Sci.* **105**, 18848–

18853 (2008).

15. J. T. Wootton, C. A. Pfister, Carbon system measurements and potential climatic drivers at a site of rapidly declining ocean pH. *PLoS ONE* **7**, e53396 (2012), doi:10.1371/journal.pone.0053396.

16. C. A. Pfister *et al.* Rapid environmental change over the past decade revealed by isotopic analysis of the California mussel in the Northeast Pacific. *PLoS ONE* **6**, e25766 (2011), doi:10.1371/journal.pone.0025766

17. R. S. Steneck, The ecology of coralline algal crusts: convergent patterns and adaptive strategies. *Ann. Rev. Ecol. Syst.* **17**, 273–303 (1986).

18. A. N. C. Morse, D. E. Morse, Recruitment and metamorphosis of *Haliotis* larvae induced by molecules uniquely available at the surfaces of crustose red algae. *J. Exp. Mar. Biol. Ecol.* **75**, 191–215 (1984).

19. L. Harrington, K. E. Fabricius, G. De'ath, A. Negri, Recognition and selection of settlement substrata determine post-settlement survival in corals. *Ecol.* **85**, 3428–3437 (2004).

20. A. D. Smith, A. A. Roth, Effect of carbon dioxide concentration on calcification in the red coralline alga *Bossiella orbigniana*. *Mar. Biol.* **52**, 217–225 (1979).

21. M. D. Johnson, V. W. Moriarty, R.C. Carpenter, Acclimatization of the crustose coralline alga *Porolithon onkodes* to variable pCO_2. *PLoS ONE* **9**, e87678 (2014), doi:10.1371/journal.pone.0087678.

22. R. S. Steneck, S. D. Hacker, M. N. Dethier, Mechanisms of competitive dominance between crustose coralline algae: an herbivore-mediated competitive reversal. *Ecol.* **72**, 938-950 (1991).

23. R.T. Paine, Ecological determinism in the competition for space. *Ecol.* **65**, 1339-1348 (1984).

24. M. N. Dethier, R.S. Steneck, Growth and persistence of diverse intertidal crusts: survival of the slow in a fast-paced world. *Mar. Ecol. Prog. Ser.* **223**, 89-100 (2001).

25. R. S. Steneck, R. T. Paine, Ecological and taxonomic studies of shallow-water encrusting Corallinaceae (Rhodophyta) of the boreal northeastern Pacific. *Phycologia* **25**, 221-240 (1986).

26. S. J. McCoy, Morphology of the crustose coralline alga *Pseudolithophyllum muricatum* (Corallinales, Rhodophyta) responds to 30 years of ocean acidification in the northeast Pacific. *J. Phycol.* **49**, 830-837 (2013).

27. C. E. Cornwall *et al.* Diurnal fluctuations in seawater pH influence the response of a calcifying macroalgal to ocean acidification. *Proc. R. Soc. B.* **280**, 20132201 (2013), doi: 10.1098/rspb.2013.2201.

28. N. A. Kamenos, A. Law, Temperature controls on coralline algal skeletal growth. *J. Phycol.* **46**, 331-335 (2010).

29. J. Chappell, Coral morphology, diversity, and reef growth. *Nature* **286**, 249-252 (1980).

30. A. Cohen *et al.* Morphological and compositional changes in the skeletons of new coral recruits reared in acidified seawater: insights into the biomineralization response to ocean acidification. *Geochem. Geophys. Geosyst.* **10**, Q07005 (2009), doi:10.1029/2009GC002411.

Figure legends

Figure 1. Thickness transects from the thallus edge towards the center of the crust for **a**, *P. muricatum* (historical N=4, modern N=6), **b**, *P. whidbeyense* (historical N=6, modern N=6), **c**, *L. impressum* (historical N=5, modern N=6), and **d**, *L. phymatodeum* (historical N=3, modern N=5). Species means for historical specimens are shown in filled circles and averages for modern specimens in empty squares. Dotted lines indicate standard error. *Data for *P. muricatum* includes a subset of previously published data in McCoy[26].

Figure 2. Comparison of **a**, inter- and **b**, intra-filament wall thicknesses for *P. muricatum* (historical N=49, modern N=47), *L. impressum* (historical N=73, modern N=73), *P. whidbeyense* (historical N=73, modern N=73), and *L. phymatodeum* (historical N=22, modern N=45). Data from historical specimens is shown in solid bars, and modern specimens in hashed bars. Error bars indicate standard error. Significant reductions in inter-filament wall thickness were found between historical and modern specimens in *P. whidbeyense* (*, p=0.022) and *L. phymatodeum* (**, p=0.025). Inset **c** shows SEM image of *Lithothamnion glaciale* showing position of intra- and inter-filament walls.

Figure 3. **a**, Mean monthly SST in °C. Blue points show data from Cape Elizabeth 1987-2012 (NOAA Buoy 46041, 47.4°N, 124.5°W; ndbc.noaa.gov), and black points data from Tatoosh Island 2000-2012 (48.4°N, 128.7°W). There was no trend in SST over time at either site. Cape Elizabeth consistently experiences daily temperatures 2-3°C higher than Tatoosh Island, and is located ~50 km to the southeast[16]. **b**, Stable isotope composition of carbon ($\delta^{13}C$) measured in *M. californianus* shells from Tatoosh Island reveal a shift in carbon system chemistry over the last

decade[16]. **c**, pH time series measured at Tatoosh Island exhibiting seasonal variation and year-to-year trends (pH decline -0.058 units/year)[14,15]. Data points show measurements every 30 min at high tide from April-September. Figure modified from McCoy and Pfister1[3].

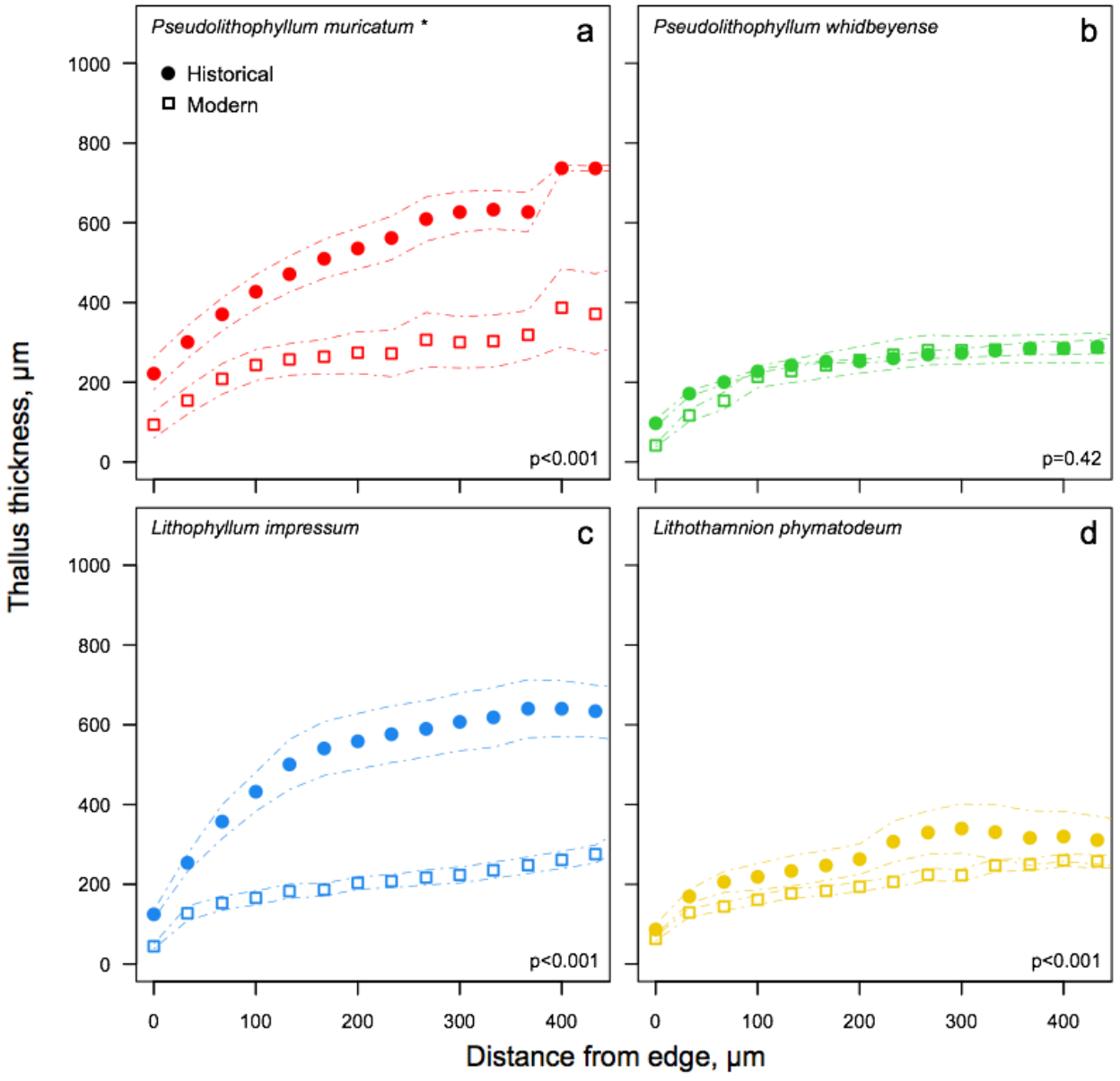

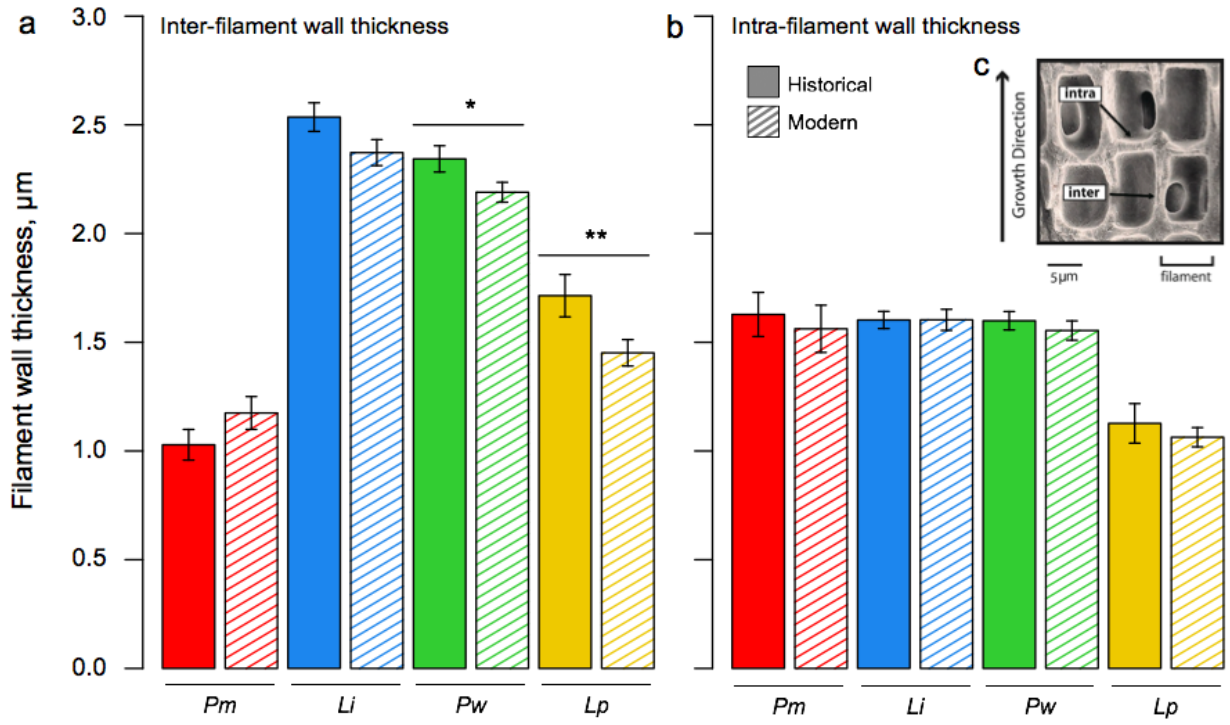
a
Inter-filament wall thickness
Filament wall thickness, µm
3.0
2.5
2.0
1.5
1.0
0.5
0.0
*
**
Pm
Li
Pw
Lp
b
Intra-filament wall thickness
Historical
Modern
c
Growth Direction
intra
inter
5µm
filament
Pm
Li
Pw
Lp

418

419

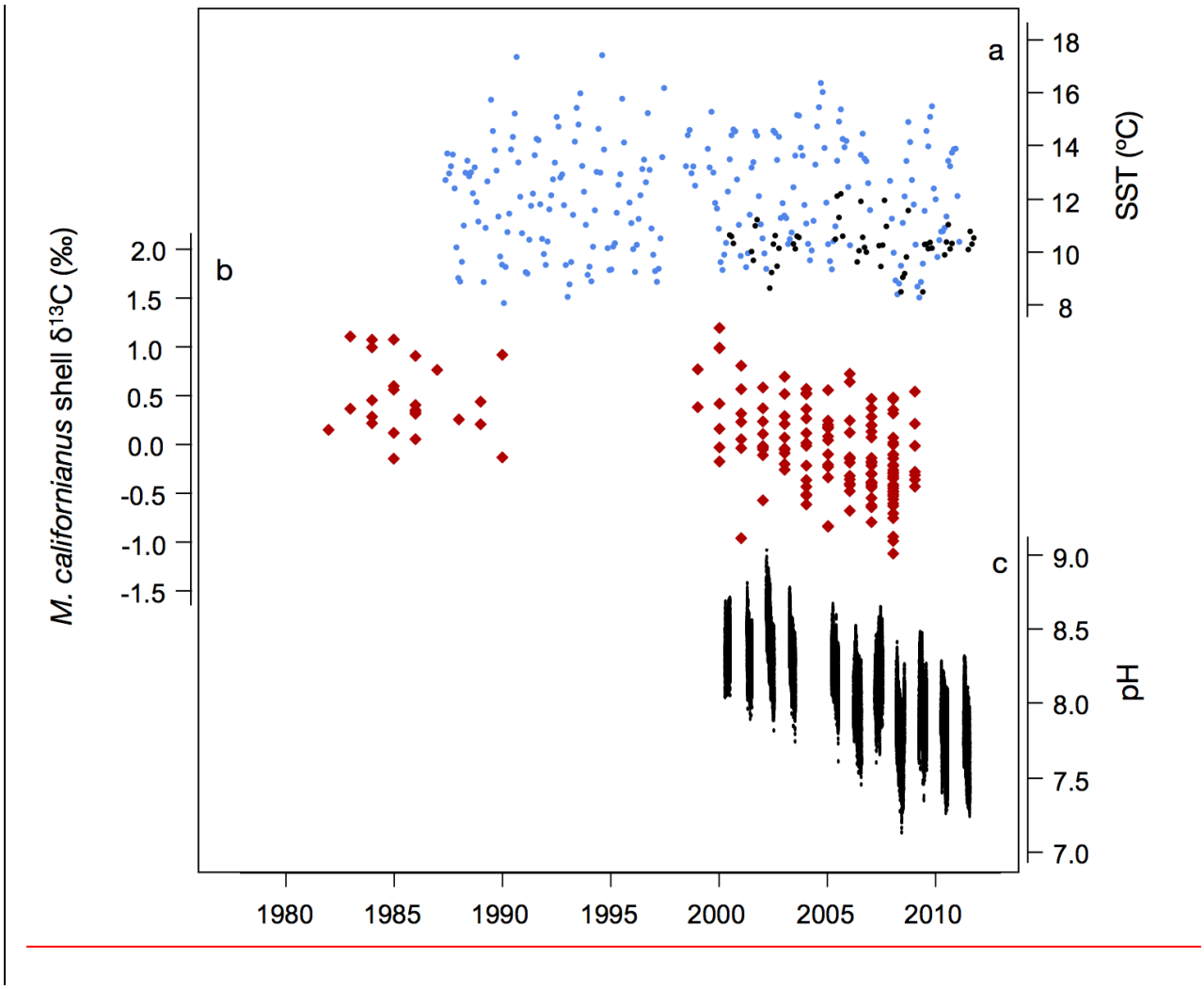
a
b
c
18
16
14
12
10
8
SST (°C)
2.0
1.5
1.0
0.5
0.0
-0.5
-1.0
-1.5
M. californianus shell δ13C (‰)
9.0
8.5
8.0
7.5
7.0
pH
1980
1985
1990
1995
2000
2005
2010

420